

# Neocarzinostatin as a Probe for DNA Protection Activity—Molecular Interaction With Caffeine

Der-Hang Chin,<sup>1\*</sup> Huang-Hsien Li,<sup>1</sup> Hsiu-Maan Kuo,<sup>2</sup> Pei-Dawn Lee Chao,<sup>3</sup> and Chia-Wen Liu<sup>1</sup>

<sup>1</sup>Department of Chemistry, National Chung Hsing University, Taichung, Taiwan, Republic of China

<sup>2</sup>Department of Parasitology, China Medical University, Taichung, Taiwan, Republic of China

<sup>3</sup>Graduate Institute of Chinese Pharmaceutical Sciences, China Medical University, Taichung, Taiwan, Republic of China

Neocarzinostatin (NCS), a potent mutagen and carcinogen, consists of an enediyne prodrug and a protein carrier. It has a unique double role in that it intercalates into DNA and imposes radical-mediated damage after thiol activation. Here we employed NCS as a probe to examine the DNA-protection capability of caffeine, one of common dietary phytochemicals with potential cancer-chemopreventive activity. NCS at the nanomolar concentration range could induce significant single- and double-strand lesions in DNA, but up to  $75 \pm 5\%$  of such lesions were found to be efficiently inhibited by caffeine. The percentage of inhibition was caffeine-concentration dependent, but was not sensitive to the DNA-lesion types. The well-characterized activation reactions of NCS allowed us to explore the effect of caffeine on the enediyne-generated radicals. Postactivation analyses by chromatographic and mass spectroscopic methods identified a caffeine-quenched enediyne-radical adduct, but the yield was too small to fully account for the large inhibition effect on DNA lesions. The affinity between NCS chromophore and DNA was characterized by a fluorescence-based kinetic method. The drug–DNA intercalation was hampered by caffeine, and the caffeine-induced increases in DNA–drug dissociation constant was caffeine-concentration dependent, suggesting importance of binding affinity in the protection mechanism. Caffeine has been shown to be both an effective free radical scavenger and an intercalation inhibitor. Our results demonstrated that caffeine ingeniously protected DNA against the enediyne-induced damages mainly by inhibiting DNA intercalation beforehand. The direct scavenging of the DNA-bound NCS free radicals by caffeine played only a minor role. *Mol. Carcinog.* © 2011 Wiley-Liss, Inc.

Key words: enediyne; free radical; intercalation

## INTRODUCTION

Research on common dietary constituents that can prevent mutagenesis and carcinogenesis is a rapidly growing area with significant health impacts. A potent mutagen and carcinogen like neocarzinostatin (NCS) [1–3] could be used as a sensitive probe to identify phytochemicals that possess potential cancer-chemopreventive activity. In particular, NCS plays a unique double role as a DNA intercalator and free radical generator [4]. With its multi-genotoxic actions well-understood at the molecular level, a probe like NCS has an advantage in that it could further our understanding about the mechanism of DNA protection.

Similar to radiation, a class of naturally occurring enediyne antibiotics [5], which belongs to some of the most potent categories discovered, also exert their biological effects through radical-mediated damage to the cellular genome. Among the known enediyne antibiotics, NCS [6] was the first to be characterized and has been studied in the most detail [4]. Chromoprotein complex of neocarzinostatin (holoNCS) is a 1:1 complex of an enediyne chromophore (neocarzinostatin chromophore [NCS-C]; MW = 659; see Scheme 1 for its

structure) and a carrier protein (apoprotein component of neocarzinostatin (apoNCS); 113 amino acids, see Ref. [7] for its primary structure) [4]. The mode-of-action of holoNCS involves the release of NCS-C [8], which then binds to the target DNA by intercalation of its naphthoate moiety [9,10]. The activity of NCS-C is triggered by thiolate attack at C-12 that irreversibly cascades down to a transient C2,6-radical species (Scheme 1) [4]. The highly reactive radical species abstracts hydrogen atoms from DNA [11,12] or solvents [13,14] to form a

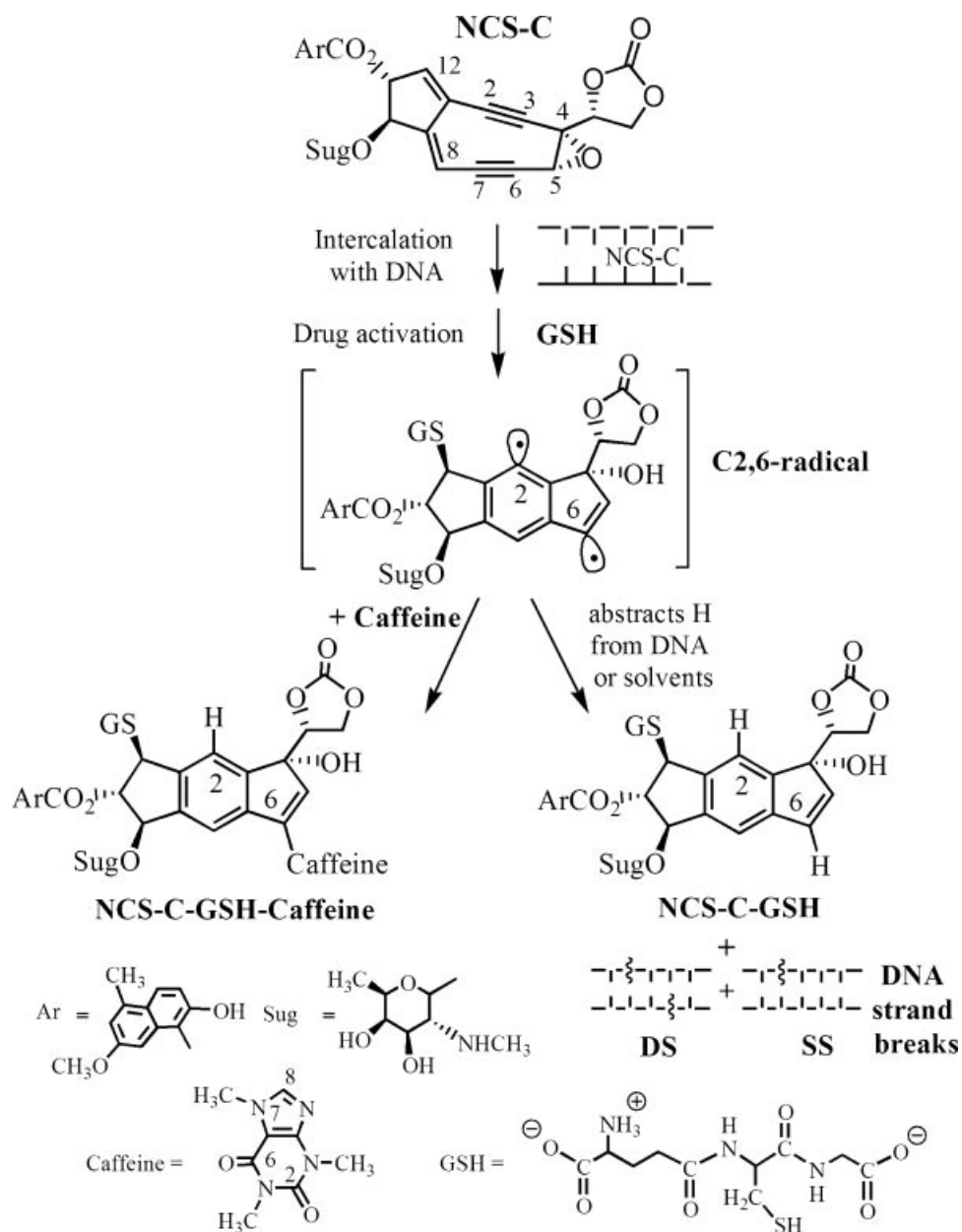
Abbreviations: NCS, neocarzinostatin; holoNCS, chromoprotein complex of neocarzinostatin; NCS-C, neocarzinostatin chromophore; apoNCS, apoprotein component of neocarzinostatin; SS, single-strand (breaks or lesions of DNA); DS, double-strand (breaks or lesions of DNA); HPLC, high-performance liquid chromatography; ct-DNA, calf-thymus DNA; GSH, glutathione; Tris, tris(hydroxymethyl)-aminomethane; TS, total strand (breaks or lesions of DNA); MS, mass spectrometry.

\*Correspondence to: Department of Chemistry, National Chung Hsing University, 250 Kuo-Kuang Road, Taichung 40227, Taiwan, Republic of China.

Received 23 October 2010; Revised 27 March 2011; Accepted 4 April 2011

DOI 10.1002/mc.20788

Published online in Wiley Online Library (wileyonlinelibrary.com).



SCHEME 1. Schematic representation of NCS-C activation and DNA damage reactions.

stable thiol-NCS-C adduct. Subsequent oxidative reactions lead to single-strand (SS) and double-strand (DS) DNA lesions [4].

Among all known phytochemicals, caffeine is arguably one of the most common dietary constituents that have potential chemopreventive activity. Coffee and tea are popular beverages throughout the world, and caffeine (1,3,7-trimethylxanthine), a typical purine alkaloid, is one of the most important components. Plants, like coffee (*Coffea arabica*), cola (*Cola nitida*), and tea (*Camellia sinensis*), use secondary metabolites such as caffeine in chemical defense against reactive

species [15]. When consumed by humans, caffeine is released and can often exert pleiotropic effects in the cellular environment. In fact, there have been a myriad of studies dealing with the physiological protection effects of caffeine (e.g., see Refs. [16–22]).

On the molecular level, caffeine has been shown to act as an effective intercalation inhibitor. Mutagens and carcinogens such as acridine orange [23,24], actinomycin [24], daunomycin [24,25], doxorubicin [26], and dimethylbenz[a]anthracene [27] have been shown to reduce their binding to DNA through interference from caffeine. In

addition to inhibiting the intercalation of planar aromatic molecules into DNA, caffeine is also known to act as an efficient free radical scavenger by quenching different types of free radicals to form various radical adducts [28–30]. It has been suggested that caffeine protects DNA from radiation by its efficient ability to scavenge highly reactive free radicals [31,32].

Interest in the effects of caffeine on the bioactivity of NCS in the cellular environment has developed since three decades ago [33–40]. Studies have suggested that the interaction between caffeine and NCS might be closely related to the cellular effects of X-ray irradiation [36]. However, no detailed mechanism has been explored, nor have any caffeine-NCS interactions on the molecular level been elucidated. Here, we aimed to study whether NCS could effectively probe the DNA-protection capability of caffeine *in vitro*. If so, does it play the role of a radical scavenger, an intercalation inhibitor, or both in its DNA-protection mechanism?

## MATERIALS AND METHODS

### Materials

NCS powder, a gift from Kayaku Co., Ltd (Itabashi-Ku, Tokyo, Japan) was dissolved in water and stored in the dark at  $-80^{\circ}\text{C}$ . The concentration of holoNCS was determined by UV absorption at the 340-nm plateau ( $\epsilon_{340} = 10\,800\ \text{M}^{-1}\ \text{cm}^{-1}$ ) [41]. The NCS-C stock was prepared by repetitive extraction from lyophilized holoNCS in 20 mM of sodium citrate (pH 4.0)/methanol and stored at  $-80^{\circ}\text{C}$  in amber glass vials [42]. Integrity of NCS-C was confirmed by high-performance liquid chromatography (HPLC) as described previously [43]. Concentration of the NCS-C stock was determined by peak integration on the HPLC profile, monitored by absorbance at 226 nm, or by the increase in  $A_{340}$  following titration into excess apoNCS using a UV/Vis spectrophotometer. Supercoiled plasmid DNA pBR322 was purified from *E. coli* DH5 $\alpha$  harboring the plasmid DNA using a Mini-Prep plasmid isolation kit (Qiagen, Inc., Hilden, Germany) [44]. Calf-thymus DNA (ct-DNA) (Sigma, St. Louis, MO) was sonicated ( $\sim 400$  bp) and purified as described in Refs. [9,42]. DNA concentration, expressed as nucleotide concentration, was determined by  $A_{260}$ . All purified DNA stock solutions had an  $A_{260/280}$  absorbance ratio of 1.8–1.9, indicating that the DNA was sufficiently free of protein. Caffeine and all other reagents obtained were of analytical grade.

### NCS-Induced DNA Lesion Reactions and Analysis

The NCS-induced DNA lesions were performed with or without caffeine using either holoNCS or

NCS-C. Samples of 5–100 nM (final concentration) holoNCS or NCS-C were added to 100–3500 ng of the supercoiled pBR322 containing 4.25 mM of ammonium acetate (pH 4.0), 3 mM of EDTA (pH 4.0), 5 mM of glutathione (GSH), and caffeine (for a final concentration range of 0–10 mM). Tris(hydroxymethyl)-aminomethane (Tris)-HCl (pH 7.4) at a final concentration of 100 mM was added last to initiate the NCS-DNA reaction. The final volume of each sample was 18  $\mu\text{L}$  with methanol content of 10% (v/v) or below (resulting from the methanolic NCS-C stock). Samples were incubated for 30 min in the dark at  $37^{\circ}\text{C}$  for the holoNCS-mediated DNA lesion reactions, and  $0^{\circ}\text{C}$  for the NCS-C reactions. To convert all abasic site lesions to DNA strand breaks and assess the total DNA lesions, putrescine at pH 8.0 was added at a final concentration of 100 mM after the NCS-DNA reactions. Samples were further incubated for 1 h at  $25^{\circ}\text{C}$  prior to analysis [42,45].

The NCS-cleaved DNA fragments were analyzed on a 1% agarose gel containing ethidium bromide (0.5  $\mu\text{g}/\text{mL}$ ) in a mini electrophoresis apparatus (Hoefer Scientific Instrument, San Francisco, CA) and were documented with an Alpha Imager 2000 (Alpha Innotech Corp., San Leandro, CA). Fractions of supercoiled (form I), relaxed circular (form II), and linear duplex (form III) DNA were estimated by integration of their respective bands. Since form I stained at 70% of forms II and III with ethidium bromide, its fluorescence intensity was corrected. The number of total strand (TS) breaks per DNA molecule,  $N_{\text{TS}}$ , was calculated from the fraction of remaining form I ( $f_{\text{I}}$ ) following the Poisson distribution:  $N_{\text{TS}} = -\ln(f_{\text{I}}/[f_{\text{I}}]_0)$ , where  $[f_{\text{I}}]_0$  is the fraction of form I in the control [42,45,46]. The number of DS breaks,  $N_{\text{DS}}$ , was calculated from the fraction of remaining form III ( $f_{\text{III}}$ ) by the following equation:  $\ln(N_{\text{DS}}) - N_{\text{DS}} = \ln(f_{\text{III}}/[f_{\text{I}}]_0)$ . The number of SS breaks,  $N_{\text{SS}}$ , was calculated from the difference between TS and DS:  $N_{\text{SS}} = N_{\text{TS}} - N_{\text{DS}}$  [42,46].

### Activation Reaction of NCS-C and Its Analyses

The thiol-induced activation reaction of NCS-C was performed in the presence and absence of ct-DNA both with and without caffeine. In the absence of DNA, a series of samples of GSH-activated NCS-C reaction in a final volume of 100  $\mu\text{L}$  were prepared by mixing 5 mM of GSH, 4.5 mM of ammonium acetate (pH 4), and 3 mM of EDTA (pH 4) with a specified amount of NCS-C (10–39  $\mu\text{M}$ ) in the presence of various concentrations of caffeine (0–60 mM). Each reagent was precooled to  $0^{\circ}\text{C}$ , and Tris-HCl (pH 8.0) was added last at a final concentration of 100 mM to initiate the activation reaction. The methanol content was kept constant at 5% (v/v). The samples were incubated at  $0^{\circ}\text{C}$  for 5 min prior to HPLC analysis.

In the presence of DNA, analyses were performed at NCS-C concentration level either 10  $\mu\text{M}$  or 100 nM. At 10  $\mu\text{M}$ , samples of NCS-C were added to ct-DNA at a DNA nucleotide phosphorus to drug molar ratio (P:D) of 10 (100  $\mu\text{M}$ ), and were mixed with caffeine (0–10 mM), GSH (5 mM), EDTA (3 mM, pH 4), ammonium acetate (4.5 mM, pH 4), and Tris-HCl (100 mM, pH 8.0) (final volume, 100  $\mu\text{L}$ ). The methanol content was kept constant at 5% (v/v). Samples were incubated at 0°C for 3 h. DNA was then removed by precipitation in 70% ethanol containing 0.3 M sodium acetate. The filtrates were lyophilized to dryness to remove excess ethanol and re-dissolved in water prior to chromatographic analysis. When the activation reaction was carried out at a concentration level of 100 nM of NCS-C, volume was increased to 10 mL. Samples of NCS-C were mixed with ct-DNA (10  $\mu\text{M}$ ), caffeine (0–10 mM), GSH (2 mM), EDTA (0.3 mM, pH 4), and Tris-HCl (10 mM, pH 8.0). The methanol content resulted from the methanolic NCS-C stock was 0.042% (v/v). The reaction mixtures were incubated at 0°C for 30 min. Each solution was then lyophilized to reduce the volume to about 0.5–1 mL before DNA was precipitated by 70% ethanol containing 0.3 M sodium acetate. The filtrates were lyophilized to dryness and re-dissolved in water prior to HPLC analysis.

A Waters Millennium HPLC (Milford, MA) equipped with a model 600E solvent delivery system, a 996 photodiode array detector, and either a Waters 474 or a Jasco FP-1520 (Tokyo, Japan) fluorescence detector was used for the drug activation product analyses. Separations were carried out on a Waters  $\mu$ -Bondapak reverse phase C18 column (particle size, 10  $\mu\text{m}$ ; pore size, 125 Å; 0.39 cm  $\times$  30 cm) with a 0.4 cm guard column. All samples were eluted with H<sub>2</sub>O/CH<sub>3</sub>OH gradient containing 5 mM of ammonium acetate at pH 4. NCS-C and its products were characterized and identified by previously established methods [43].

#### Mass Analyses

All mass measurements were performed on a Finnigan LCQ mass spectrometry detector (Thermo Electron, San Jose, CA) equipped with an atmospheric pressure ionization source using electrospray ionization (ESI) (+)-charge mode. Samples isolated from HPLC (in approximately 50–70% CH<sub>3</sub>OH/H<sub>2</sub>O containing 5 mM of ammonium acetate at pH 4) were directly infused for mass measurement. Data were acquired from 150 to 2000  $m/z$  in profile mode at a flow rate of 3–10  $\mu\text{L}/\text{min}$ . The mass spectrometry (MS) MS/MS fragmentation patterns of the isolated NCS-C activation products were analyzed in the data-dependent acquisition MS/MS (MS<sup>n</sup>) mode, in which the most intense ions detected in the precursor MS scan were selected for collision-induced dissociation.

Fragmentation data were acquired in the 200–1000  $m/z$  range in centroid mode using a normalized collision energy setting of approximately 25%. The deviation of all measured  $m/z$  ratios was typically <0.03%.

#### NCS-C–DNA Binding Study

Binding affinity of NCS-C to ct-DNA was estimated using NCS-C degradation kinetics in the absence and presence of DNA, monitored by a SLM-Aminco Bowman series 2 Luminescence Spectrofluorimeter (SLM Aminco Bowman, Urbana, IL). Samples at a final volume of 150  $\mu\text{L}$  were prepared by mixing different concentrations of caffeine (0–10 mM), 20 mM of phosphate buffer (pH 7), and 1  $\mu\text{M}$  of NCS-C in the absence or presence of 100  $\mu\text{M}$  of ct-DNA (P:D, 100). The methanol content was kept constant at 5% (v/v) in all samples. After excitation at 380 nm, the emission at 490 nm was recorded in time-scan mode until it reached a plateau. The remaining concentration of NCS-C ([NCS-C]) was determined by the following equation:  $[\text{NCS-C}] = [\text{NCS-C}]_0 - \{F_t/(F_\infty - F_0)\} \times [\text{NCS-C}]_0$ . In the equation,  $[\text{NCS-C}]_0$  is the initial concentration;  $F_t$  is the measured fluorescent emission at time  $t$ ;  $F_0$  is the initial reading; and  $F_\infty$  is the plateau reading. For each specific concentration of caffeine, NCS-C degradation rates were measured both with and without DNA. The first-order rate constant in the absence ( $k_0$ ) and presence ( $k_{\text{DNA}}$ ) of ct-DNA were determined by the slope of a linear plot of logarithmic [NCS-C] versus time. The apparent equilibrium dissociation constant ( $K_d$ ) of the NCS-C–DNA binding complex was determined by the derived equation [10]:  $K_d = [\text{DNA}]_f^*/((k_0/k_{\text{DNA}}) - 1)$ , where  $[\text{DNA}]_f^*$  corresponds to the concentration of free binding site on DNA. Since there are 0.125 high affinity NCS-C binding sites per nucleotide,  $[\text{DNA}]_f^*$  is equivalent to 0.125 times of the total DNA nucleotide concentration [10].

## RESULTS

### NCS-Induced DNA Lesions Were Efficiently Inhibited by the Presence of Caffeine

The ability of NCS to induce DNA damage is known to vary with the structure of an applied thiol activator [42,45], and the variation can be as large as threefold [42]. Also, NCS-induced DNA SS lesions are predominant over DS ones, but the DS type is more lethal and has been correlated with cell death in human tumors [4,47]. After careful assessment of all known thiol activators for this caffeine-related DNA damage study, we chose to use GSH, which is the most abundant eukaryotic cellular thiol. GSH not only efficiently activates NCS to induce a high-level of TS DNA lesions, but, more importantly, it is also the most effective thiol known to produce lethal DS lesions [45].

After hydrogen abstraction, the NCS-induced DNA lesions can be oxidized to form either direct strand breaks or abasic sites. The abasic site lesions, although minor in occurrence, could not be ignored because they contribute to a significant portion of the lethal DS lesions [45]. For this reason, we converted all abasic site lesions into strand breaks by further putrescine treatment [42], which cleaves strands at virtually all abasic sites [48]. The DNA fragments that resulted from strand breaks were then resolved in agarose gel electrophoresis. The number of TS, SS, and DS strand breaks were analyzed by following the Poisson distribution [46] in the conversion of supercoiled DNA (form I) into relaxed circular (form II) and linear duplex (form III) forms. Without added caffeine, the number of SS, DS, and TS breaks per nM NCS obtained in the present study were comparable to known values [44,45], confirming the validity of the employed analytical method.

Electrophoretic analyses revealed that the addition of caffeine markedly reduced the NCS-mediated DNA strand breaks. Figure 1 shows some of the gel images obtained from reactions of holoNCS and NCS-C at 10 and 100 nM. To compare inhibition efficiencies for the different types of lesions, we expressed the caffeine-induced inhibition of DNA strand breaks as a percentage of the controlled data without caffeine. The number of different types of DNA scissions, SS, DS, or TS, in the absence of caffeine was normalized to 100 and set as 0% inhibition. Figure 2a shows the percent inhibition of TS lesions induced by 10 nM of NCS measured over a wide range of caffeine concentrations. The inhibition effect was small at a caffeine concentration below 1 mM, but increased sharply above 1 mM. DNA scission activity from NCS was largely suppressed by caffeine up to  $75 \pm 5\%$  at a concentration of 10 mM, where the inhibition effect gradually leveled off. When the drug concentration was increased to 100 nM (see Figure 1c), the inhibition of DNA damage reduced to  $60 \pm 5\%$  and showed no leveling off effect at 10 mM of caffeine. The results implied a competition for DNA between caffeine and the drug. Because DNA damage was mediated by the NCS-generated C2,6-free radicals (see Scheme 1), the data suggest that caffeine could efficiently protect DNA from the enediyne-generated active radicals.

The present electrophoresis results revealed that the caffeine-induced inhibition of DNA damage was similar in both holoNCS and NCS-C when the drug concentration was 10 nM (see Figure 2a), suggesting insensitivity to the drug form at the nanomolar concentration range, although caffeine stimulated NCS-C release from 10  $\mu$ M of holoNCS (data not shown). When the NCS-induced DNA TS breaks were classified into SS and DS, both showed very similar trends with increasing caffeine

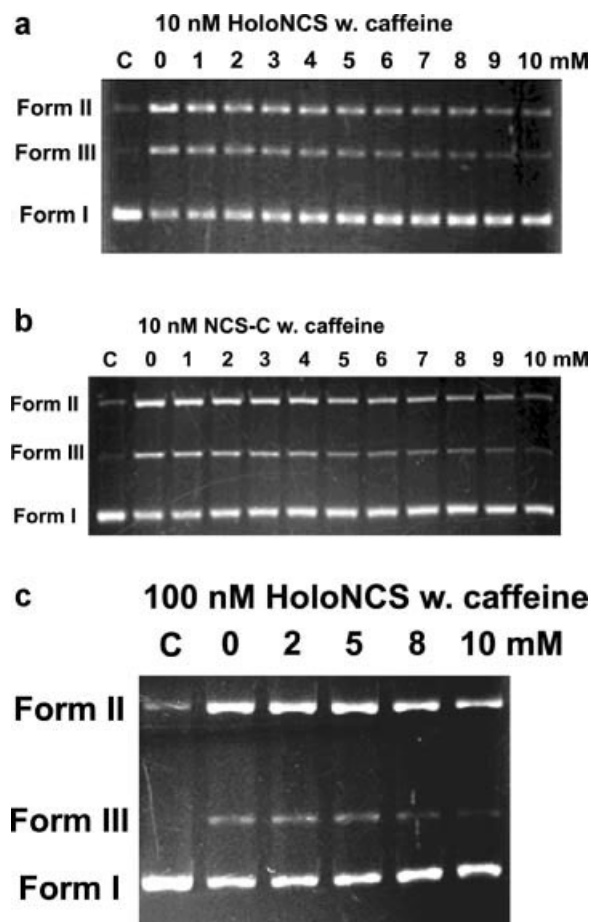


Figure 1. Agarose gel electrophoresis of ethidium bromide stained pBR322 DNA after treatment with NCS. (a) Samples of 10 nM of holoNCS were mixed with 200 ng of DNA containing ammonium acetate (4.25 mM, pH 4), EDTA (3 mM, pH 4), GSH (5 mM), and (0–10 mM) caffeine. Tris-HCl (100 mM, pH 7.4) was added last and the reaction mixtures were incubated at 37°C for 30 min. Samples were then treated with putrescine (100 mM, pH 8.0) at 25°C for 1 h before analyses. (b) Conditions were the same as in (a), except that holoNCS was replaced by NCS-C and samples were incubated at 0°C for 30 min before putrescine treatment. The methanol content in each sample was 10% (v/v). (c) Conditions were the same as in (a), except that 100 nM of holoNCS and 3500 ng of DNA were used for each sample. After putrescine treatment, an aliquot of each sample that was equivalent to 200 ng of DNA was taken for electrophoretic analysis.

concentrations and no significant differences in percent inhibition were found between the two types of lesions (see Figure 2, panel b and c). These results suggest that the inhibition mechanism of caffeine did not affect the type of DNA lesion produced by the activated NCS.

#### Caffeine Was Able to Quench the Thiol-Activated Enediyne Radical Species

NCS is a prodrug [5] that needs to be activated by a thiol to generate a highly active C2,6-radical species (Scheme 1). This bioactive species abstracts a hydrogen at C2 and C6 and transforms into a postactivated thiol-drug adduct (see NCS-C-GSH

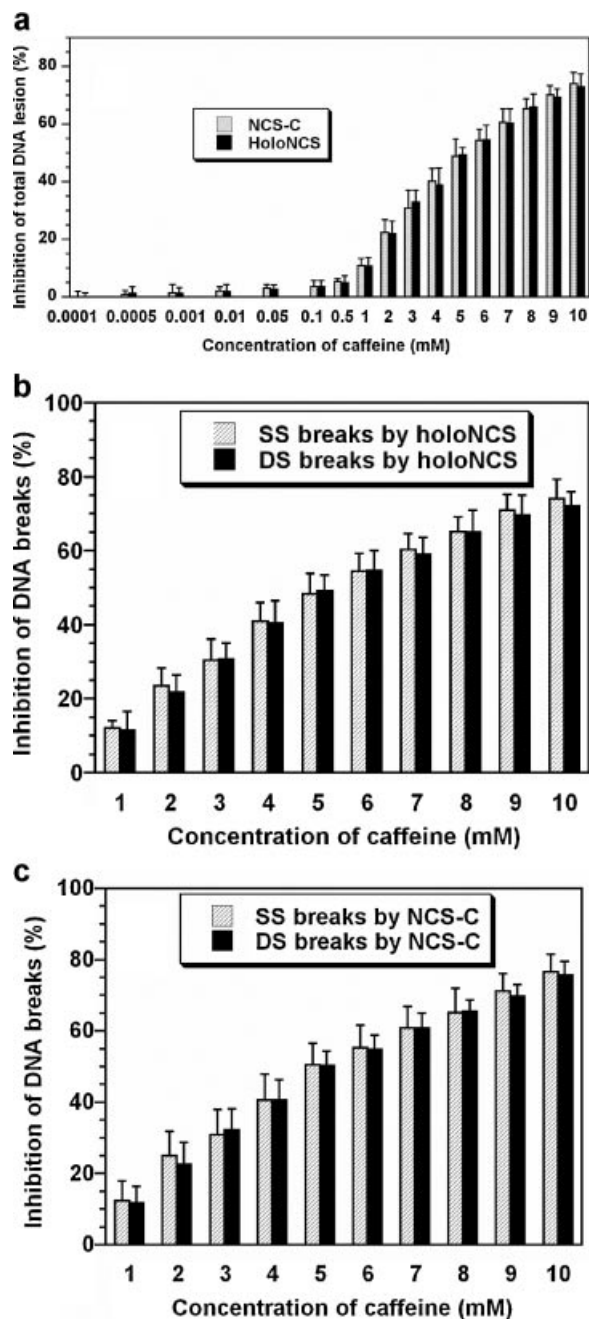


Figure 2. Effect of caffeine on the NCS-mediated DNA lesions. (a) Inhibition of TS breaks of DNA induced by holoNCS (black bar) and NCS-C (hatched bar) in the presence of caffeine. (b) Inhibition of holoNCS-induced SS (hatched bar) and DS (black bar) breaks of DNA by the presence of caffeine. (c) Inhibition of NCS-C-induced SS (hatched bar) and DS (black bar) breaks of DNA by the presence of caffeine. The holoNCS- and NCS-C-induced DNA damage reactions were performed at 37°C and 0°C, respectively. The drug concentration used was 10 nM and NCS-DNA reactions were activated by GSH at pH 7.4 in the presence of caffeine between 0.1  $\mu$ M and 10 mM. The NCS-induced DNA lesions were all converted to strand breaks by treating with 100 mM of putrescine at pH 8.0 and 25°C for 1 h. All DNA fragments were analyzed by electrophoresis. The percent inhibition was estimated based on a controlled experiment without caffeine. All values were obtained from an average of a minimum of three repetitions. The cap on each bar represents standard deviation.

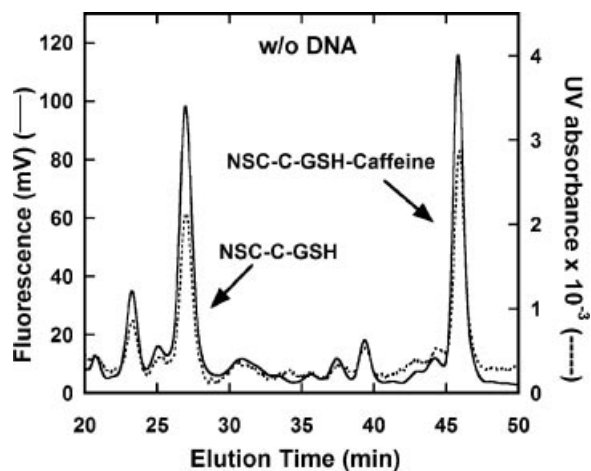
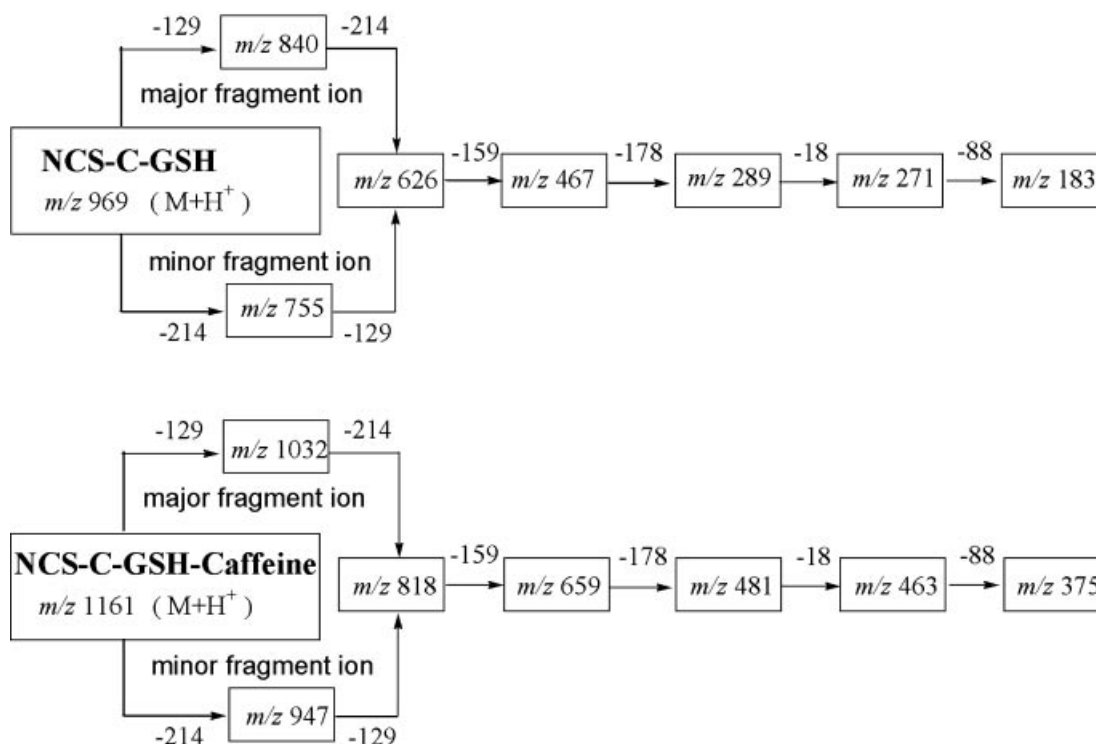


Figure 3. NCS-C activation in the presence of caffeine without DNA. The postactivation products from the GSH-activated NCS-C reaction were analyzed by HPLC. The profiles were monitored by fluorescence emission (—) at 440 nm (excitation wavelength, 340 nm) and UV-Vis absorption (---) at 340 nm. The activation reaction of NCS-C (39  $\mu$ M) was induced by GSH (5 mM) and performed in the presence of caffeine (60 mM) at pH 8.0 and 0°C in a 100- $\mu$ L aqueous solution containing 5% (v/v) methanol.

in Scheme 1), which is stable and can be identified by the established chromatographic and spectroscopic assignments [43]. Thus, analyses of the postactivated NCS products were a reasonable approach to understand the quenching process of C2,6-radicals. Without caffeine, only one major postactivated product, NCS-C-GSH, was found in the HPLC chromatograms at 27 min (data not shown), which was consistent with the previous report [49]. The formation of NCS-C-GSH was further confirmed by UV spectroscopy [43] and mass measurement. In the presence of caffeine, an additional product was observed at 46 min in the chromatograms (Figure 3). This additional product was formed at the expense of NCS-C-GSH, and its yield was caffeine-concentration dependent, suggesting that caffeine could quench the C2,6-radical species to form a caffeine-drug adduct. This caffeine-induced, postactivated NCS product exhibited an intense fluorescence emission band at 440 nm similar to that of NCS-C-GSH. It also showed a strong UV absorption  $\beta$ -band at 226 nm, which is a characteristic feature for all postactivated derivatives of NCS-C [43]. MS identified it as a mono-caffeine adduct of NCS-C, with a  $m/z$  of 1161 that matched the theoretical ( $M + H^+$ ) value of NCS-C-GSH-caffeine (Scheme 1 and Figure 4).

Interestingly, even though activation of NCS-C generated a C2,6-radical species, only a mono-caffeine adduct was detected. No di-caffeine adduct of NCS-C was detected, even in the presence of 60 mM of caffeine, a 1500-fold excess concentration of NCS-C. Presumably, addition of a thiolate group at C12 of the bicyclic enediyne core after activation of NCS-C (Scheme 1) could

### a MS/MS data



### b Proposed fragmentation

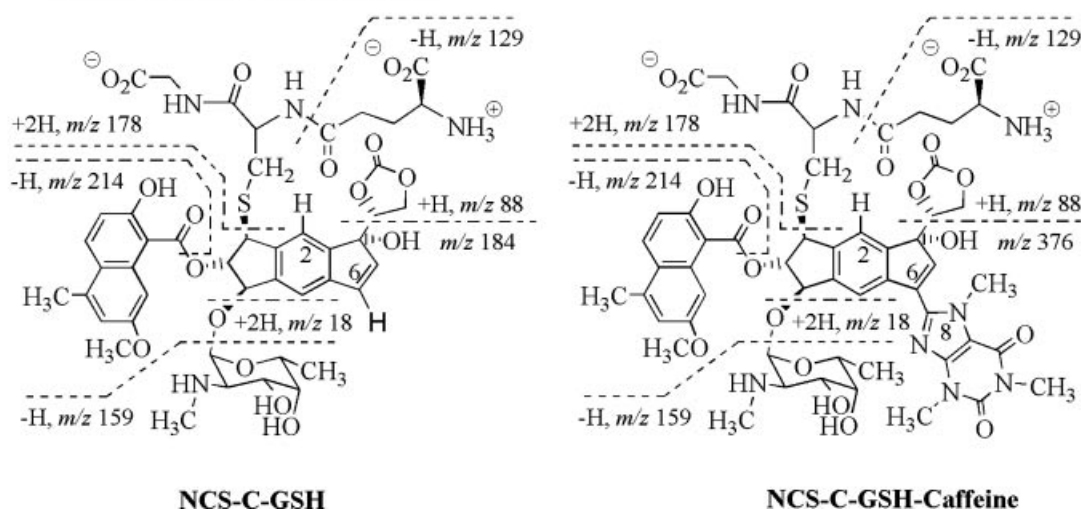


Figure 4. MS/MS fragmentation analyses of the NCS-C activation products. (a) Sequential MS/MS analyses of NCS-C-GSH and NCS-C-GSH-caffeine adducts. Both NCS-C products were isolated by HPLC and subjected to multistage  $MS^n$  analyses. The first stage collision of both products produced two intense ions. Both the major and minor fragment ions were selected as precursor ions for further fragmentation. The  $m/z$  values of the ( $M + H^+$ ) ions are shown in boxes. (b) Structural fragmentation analyses of the postactivation products, NCS-C-GSH, and NCS-C-GSH-caffeine.

effectively shield the nearby C2-radical from attack by large molecules like caffeine. A similar reaction of methyl thioglycolate with the activated C2,6-radical of NCS-C has also been reported [50]. The addition of methyl thioglycolate occurs only at

C6-, but not at the C2-radical. GSH is a tri-peptide thiol with a considerably large molecular size. Conceivably, the C6 position of the thiol-activated C2,6-radical species was much less sterically hindered and more accessible to caffeine attacks than

C2. On the other hand, the C8 position of the caffeine purine ring has been shown to be the most active site, forming numerous radical adducts with different types of free radicals [28–30,51]. Thus, a C8-substituent of caffeine at the C6 of NCS-C was expected to form the mono-caffeine adduct NCS-C-GSH-caffeine. Figure 4 shows the MS/MS fragmentation pattern of NCS-C-GSH-caffeine, which was very similar to that of NCS-C-GSH. This indicates that there was a close similarity in structure between these two postactivated NCS adducts.

#### Radical Quenching Efficiency Was Not Comparable to the DNA-Protection Effect

Although we demonstrated that caffeine was able to quench the active C2,6-radical generated by activation of the unbound NCS-C, whether this radical quenching resulted in inhibition of the NCS-induced DNA lesions still needed to be carefully evaluated. We performed the same GSH-induced activation reaction with NCS-C in an environment that allowed NCS-C to interact with DNA. Caffeine was added at a concentration range of 1–10 mM, levels at which it was found to have an obvious protection effect against NCS-induced DNA damage (Figures 1 and 2). When the activation reaction was performed with 10  $\mu$ M of NCS-C, NCS-C-GSH was found to be the major activation product with similar yields regardless of increasing the applied caffeine concentration (Figure 5a). The yield of the caffeine-quenched postactivated adduct, NCS-C-GSH-caffeine, was considerably smaller than that of the major product, NCS-C-GSH. Production of NCS-C-GSH-caffeine was barely detectable at 1 mM of caffeine. Interestingly, an  $11 \pm 3\%$  inhibition of the NCS-induced DNA lesions could be clearly detected at the same concentration level of caffeine (Figure 2). As determined by peak area integration at  $A_{226}$  [43], the yield ratios of the caffeine-quenched NCS-C-GSH-caffeine to the caffeine-unquenched NCS-C-GSH were only  $3 \pm 1\%$  and  $9 \pm 2\%$  in the presence of 5 and 10 mM of caffeine, respectively. At these same concentration levels, caffeine caused an inhibition of  $49 \pm 4\%$  and  $75 \pm 5\%$ , respectively, in the NCS-induced DNA lesions. The efficiency of quenching the activated C2,6-radical of NCS by caffeine was far from comparable to that of protecting DNA, suggesting that quenching radicals was only the minor, but not its primary, mechanism to reduce NCS-induced DNA lesions.

Because NCS is very potent in damaging DNA, the concentration of NCS required to induce estimable DNA strand breaks was in the nanomolar range (see Figures 1 and 2). However, the postactivated drug adducts analyses (shown in Figure 5a) were carried out at a drug concentration level of 10  $\mu$ M. Whether the results of HPLC could correlate to that of the electrophoretic analyses was a

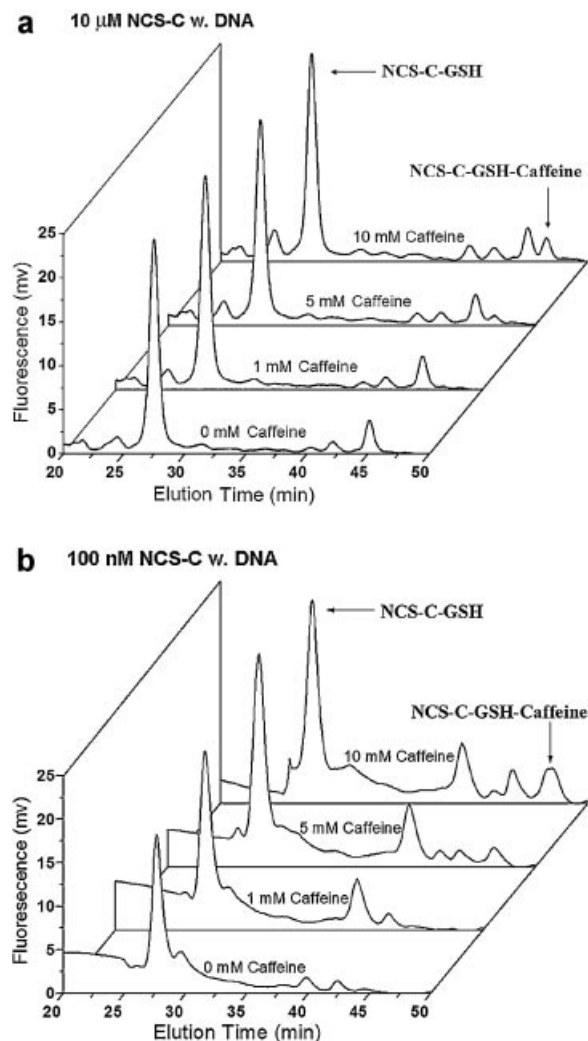


Figure 5. Effect of caffeine on NCS-C activation in the presence of DNA. (a) Samples of 10  $\mu$ M NCS-C in 100  $\mu$ L of solutions containing 100  $\mu$ M ct-DNA were mixed with 5 mM GSH and 0–10 mM caffeine at pH 8.0 and 0°C. The methanol content was kept constant at 5% (v/v). (b) Samples of 100 nM NCS-C in 10 mL of solutions containing 10  $\mu$ M ct-DNA were mixed with 2 mM GSH and 0–10 mM caffeine at pH 8.0 and 0°C. Samples were lyophilized to reduce the volume and DNA was removed by precipitation. Filtrates were lyophilized to dryness and re-dissolved in water prior to HPLC analyses. The elution profiles were monitored by fluorescence emission at 440 nm (excited at 340 nm).

concern because of the large drug concentration difference. To eliminate the effect of drug level on analyses, we managed to perform the activation reaction in 100-fold diluted NCS-C samples, in which the drug level was the same to that used in the electrophoretic analyses shown in Figure 1c. The overlain HPLC elution profiles obtained from 10 mL reactions of 100 nM of NCS-C illustrated that NCS-C-GSH remained as a major activation product in the presence of 0–10 mM of caffeine (Figure 5b). The yield ratios of the caffeine-quenched NCS-C-GSH-caffeine to NCS-C-GSH were about  $20 \pm 3\%$  in 10 mM of caffeine,



whereas an inhibition of  $60 \pm 5\%$  in the NCS activity was observed when the NCS-mediated DNA lesions was examined at the same concentration level of the drug (100 nM) and caffeine (10 mM) (Figure 1c). The results confirmed that the ability of caffeine to scavenge the enediyne-generated free radicals played only a minor role in protection of DNA.

#### Caffeine Inhibited NCS-C Binding to DNA

Because NCS-C binds to DNA prior to undergoing the thiol-induced drug activation process [45], both quenching of the active C2,6-radical and inhibition of the binding of NCS-C to DNA could protect DNA. To clarify whether or not caffeine could inhibit the intercalation of NCS-C with DNA, we measured changes in the binding affinity of NCS-C to DNA in the presence of caffeine. Because NCS-C is very labile, an indirect assay for measuring association constant of NCS-C and DNA has been developed by comparing the NCS-C degradation rate constant in the absence ( $k_0$ ) and presence ( $k_{\text{DNA}}$ ) of DNA [9,10]. Unbound NCS-C has a pronounced tendency to degrade in an aqueous environment, whereas DNA affords evident protection of NCS-C through binding [9]. Binding affinity of NCS-C and DNA can thus be fairly estimated by kinetic changes of the NCS-C degradation from absence to presence of DNA [10]. Without interference from caffeine, the obtained equilibrium dissociation constant ( $K_d$ ) for the NCS-C–DNA binding complex at pH 7 and 25°C was  $1.0 \pm 0.1 \mu\text{M}$ , which was reasonably close to the reported value of  $10^{-6} \text{ M}$  [4]. In the presence of caffeine, degradation rate of NCS-C decreased noticeably in the absence of DNA, suggesting that caffeine was able to protect the unbound NCS-C from degradation to some extent. The obtained  $K_d$  value, derived from the measured  $k_0$  and  $k_{\text{DNA}}$ , showed an increase with increasing caffeine concentration. Figure 6 demonstrates a good linear correlation between the observed  $K_d$  and caffeine concentration (correlation coefficient  $R = 0.99906$ ). Each additional mM increase in caffeine concentration raised the  $K_d$  value by  $0.15 \mu\text{M}$ , suggesting that caffeine could efficiently weaken the binding affinity between NCS-C and DNA. Examination of the NCS-C–DNA binding property revealed an increase in  $K_d$  of approximately 2.5-fold at 10 mM of caffeine compared to the value obtained without caffeine. Such an increase was comparable to the caffeine-produced reduction in NCS-induced DNA lesions. The results suggest a close correspondence of the caffeine-inhibited drug activity with the caffeine-weakened drug–DNA binding affinity. Inhibition of NCS-C intercalation with DNA by caffeine was apparently the primary protecting factor against NCS-induced DNA damage.

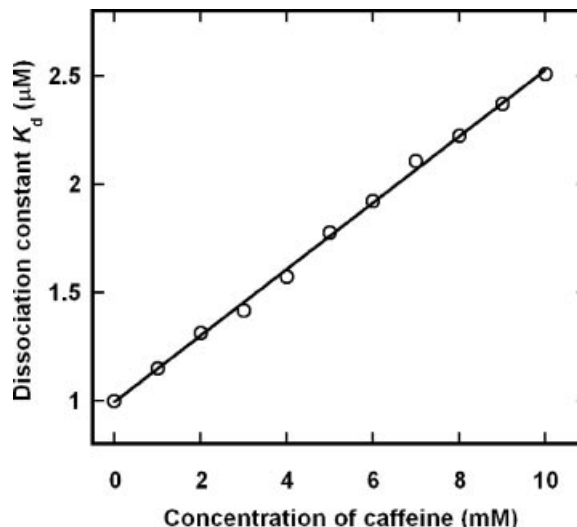


Figure 6. Effect of caffeine on NCS-C–DNA binding. Correlation between the concentration of caffeine and the equilibrium dissociation constant ( $K_d$ ) of the NCS-C–DNA binding complex obtained at pH 7 and 25°C.

#### DISCUSSION

Caffeine has been shown to repress tumor progression in rats [16,17], inhibit chemical carcinogenesis in mouse skin [18], act as a cancer preventive agent in benzo[a]pyrene-induced lung tumors in mice [19], and provide substantial protection against radiation-induced damage in mice [20,21] and mammalian cells [22]. It is also known to protect DNA from cytotoxic compounds such as ethidium bromide [24,52,53]. With its potential cancer-chemopreventive activity, we chose caffeine as a representative dietary component to study its molecular interaction with NCS. Early in vivo studies show somewhat diverse results in the influence of caffeine on the biological activity of NCS, ranging from no effect [33,39] to inhibition [36–38,40], or even enhancement [34,35]. This reflects the very complex nature in cellular interaction between caffeine and NCS. In contrast to our in vitro observation, Iseki et al. [36] reported that NCS-induced SS DNA breaks in cells were not inhibited by caffeine. In a cell the NCS-induced SS DNA breaks are known to be rapidly repaired [4,54]. In vitro studies show that the NCS-induced nascent damage in DNA can not be fixed in the absence of oxygen or a radiation sensitizer [4,55,56]. Hatayama and Yukioka [38] reported that caffeine does not aid in the repair of SS DNA breaks in cells. Whether the rapid repair system of a cell could offset the influence of caffeine on the NCS-induced SS DNA breaks is an interesting question and needs to be further investigated.

Caffeine is an effective intercalation inhibitor, but its mechanism of DNA intercalation inhibition seems quite complex. It has been shown that

caffeine can reduce the sensitivity of cells to intercalation by interfering with the cellular transport system and thereby decreasing cells' permeability to intercalators [52]. On the other hand, studies have shown various interactions among caffeine, intercalators, and DNA. Predominately through hydrophobic attraction, caffeine has been shown to interact with aromatic DNA intercalators such as ethidium bromide, acridine orange, actinomycin, and daunomycin to form noncovalent complexes [23,24,26,57]. The association of caffeine with these aromatic intercalators has been hypothesized to interfere with their intercalation into DNA [23,24]. Meanwhile, caffeine can also form a three-component complex with both the intercalator and DNA, for instance, the hetero association system of ethidium bromide-caffeine-DNA [53]. In addition to those caffeine complexes involving DNA intercalators, various modes of direct interaction between caffeine and DNA have also been suggested [25,58–61].

NMR and simulation studies on DNA binding of the stable postactivated product, NCS-C-GSH [4,62–64], suggest that formation of NCS-C-DNA binding complex is accompanied by an insertion of the naphthoate moiety in the minor grooves between two stacked base pairs. Intercalation of NCS-C has been shown to unwind the DNA helix by  $21^\circ$  and increase DNA length by  $3.3 \text{ \AA}$  [10]. Coincidentally, caffeine has also been thought to insert into [61] and unwind [59] the DNA double helix in a similar fashion. Although the exact inhibition mechanism is not clear, caffeine was likely to compete with NCS-C for DNA binding sites and thereby reduce the NCS-induced DNA lesions. In fact, formation of caffeine complexes involving DNA has been suggested to displace the bound mutagen and carcinogen molecules from DNA by competition for binding sites [24,65]. Alternatively, caffeine has been shown to bind with DNA by an arrangement of caffeine molecules outside of the DNA double helix [60]. Such an external binding of stacked caffeine molecules within the grooves of DNA could substantially block the insertion pathway of NCS-C through minor grooves. The main protection mechanism of caffeine against NCS could presumably involve caffeine competition for DNA binding sites, blocking of DNA grooves by caffeine, or both.

It is worth noting that the potent biological activity of NCS does not arise directly from intercalation of NCS-C with DNA. Rather, it is from the remarkable ability of the activated NCS-C C2,6-radical to abstract hydrogen atoms [4]. Here we demonstrated that caffeine could not compete with the vicinal DNA hydrogen atoms for the NCS-generated free radicals. However, these results should not extrapolate to a conclusion that the radical scavenging capability of caffeine was

inferior. The extremely active C2,6-radical species was very short-lived; its reaction with DNA proceeds at a very rapid rate with an estimated half-life of less than  $5 \times 10^{-6} \text{ s}$  [50]. Consequently, its reaction preference was more likely to be determined by the availability (i.e., the local distance), but not the capability (i.e., the activity), of the radical quenchers. Because NCS-C was bound to DNA, the thiol-activated C2,6-radical species would react preferentially with the surrounding hydrogen atoms of DNA rather than with the distanced caffeine molecules. As a consequence, caffeine ingeniously protected DNA by blocking the intercalation of NCS-C beforehand. Quenching the radicals by caffeine only played a minor role in protection of DNA.

Even though the physiological concentration of GSH can be high as 10 mM [66], whether the interaction between caffeine and GSH played a role in the caffeine-involved inhibition mechanism is an interesting question. Caffeine is known to reduce cellular GSH level [67,68], but seems with a relatively low efficiency compared to the DNA damage reactions induced by NCS. The GSH-activated NCS-DNA reaction in general completes within 30 min [69], whereas cells treated with caffeine show no changes in GSH level up to 2 h [67]. Furthermore, the decreased GSH level caused by caffeine might not be large enough to significantly inhibit NCS activity. A dose of 5 mM of caffeine in cells produces only up to 34% GSH reduction after a 3-h incubation [67], and 100 mg/kg in rats results in merely 22.5% reduction after 4-h treatment [68]. Although depletion of GSH results in a decrease in NCS-mediated cytotoxicity and DNA damage [69–71], only 67% decrease in NCS activity is observed when cellular GSH is reduced by more than 99.9% [69]. Considering that the optimal concentration of GSH causing maximal NCS-mediated damage in DNA is only 5 mM [45], the reduction of GSH caused by caffeine probably would not have a significant impact on NCS activity.

Our study demonstrated that caffeine, as a common dietary supplement, could protect DNA against NCS-induced lesions by up to  $75 \pm 5\%$ . NCS, an enediyne mutagen and carcinogen, plays a dual role by intercalating with DNA through its planar naphthoate moiety and also damaging DNA with its generated free radicals. We have shown that caffeine was able to quench the NCS-C radicals, but the quenching effect was considerably insignificant and only played a minor role in inhibition of DNA lesions. Rather, the DNA-binding inhibition by caffeine, which imposed restrictions on intercalation by the planar aromatic functional groups between adjacent DNA base pairs, played an important role in this detoxification process.

## ACKNOWLEDGMENTS

We thank the Kayaku Co., Ltd, for the supply of the NCS powder. Special thanks go to Ms. Chiy-Mey Huang, who made great contributions to this work by performing the HPLC and MS/MS analyses. We are also very grateful for the help from Ms. Mei-Ru Chou, who successfully made the electrophoretic and HPLC analyses at the 100 nM of drug concentration level. This work was supported by a Laboratory Grant (NHRI-EX90-8807BL) from the National Health Research Institutes and Individual Grants (95-2311-B-005-012-MY3 and 95-2113-M-005-007-MY3) from the National Science Council, Taiwan, Republic of China. This work was also supported in part by the Ministry of Education, Taiwan, Republic of China, under the ATU plan to National Chung Hsing University.

## REFERENCES

- Ishida N, Miyazaki K, Kumagai K, Rikimaru M. Neocarzinostatin, an antitumor antibiotic of high molecular weight. Isolation, physicochemical properties and biological activities. *J Antibiotics (Tokyo)* 1965;18:68–76.
- Tatsumi K, Nishioka H. Mutagenicity of an antitumor protein, neocarzinostatin, in *Escherichia coli*. *Mutat Res* 1977;56:91–94.
- Tatsumi K, Nishioka H. Effect of DNA repair systems on antibacterial and mutagenic activity of an antitumor protein, neocarzinostatin. *Mutat Res* 1977;48:195–203.
- Goldberg IH. Mechanism of neocarzinostatin action: Role of DNA microstructure in determination of chemistry of bistranded oxidative damage. *Acc Chem Res* 1991;24:191–198.
- Jones GB, Fouad FS. Designed enediyne antitumor agents. *Curr Pharm Des* 2002;8:2415–2440.
- Edo K, Mizugaki M, Koide Y, et al. The structure of neocarzinostatin chromophore possessing a novel bicyclo[7,3,0]dodecadiyne system. *Tetrahedron Lett* 1985;26:331–334.
- Sakata N, Minamitani S, Kanbe T, Hori M, Hamada M, Edo K. The amino acid sequence of neocarzinostatin apoprotein deduced from the base sequence of the gene. *Biol Pharm Bull* 1993;16:26–28.
- Jung G, Kohnlein W. Neocarzinostatin: Controlled release of chromophore and its interaction with DNA. *Biochem Biophys Res Commun* 1981;98:176–183.
- Povirk LF, Goldberg IH. Binding of the nonprotein chromophore of neocarzinostatin to deoxyribonucleic acid. *Biochemistry* 1980;19:4773–4780.
- Povirk LF, Dattagupta N, Warf BC, Goldberg IH. Neocarzinostatin chromophore binds to deoxyribonucleic acid by intercalation. *Biochemistry* 1981;20:4007–4014.
- Charnas RL, Goldberg IH. Neocarzinostatin abstracts a hydrogen during formation of nucleotide 5'-aldehyde on DNA. *Biochem Biophys Res Commun* 1984;122:642–648.
- Chin D-H, Zeng CH, Costello CE, Goldberg IH. Sites in the diyne-ene bicyclic core of neocarzinostatin chromophore responsible for hydrogen abstraction from DNA. *Biochemistry* 1988;27:8106–8114.
- Chin D-H, Goldberg IH. Internal hydrogen abstraction by activated neocarzinostatin: Quenching of the radical at C2 by hydrogen-atom transfer from the alpha-carbon of the adducted thiol. *J Am Chem Soc* 1992;114:1914–1915.
- Chin D-H, Goldberg IH. Sources of hydrogen abstraction by activated neocarzinostatin chromophore. *Biochemistry* 1993;32:3611–3616.
- Wink M. A short history of alkaloids. In: Roberts MF, Wink M, editors. *Alkaloids: Biochemistry, ecology, and medical applications*. New York: Plenum Press; 1998. pp. 11–44.
- Nishikawa A, Furukawa F, Imazawa T, Ikezaki S, Hasegawa T, Takahashi M. Effects of caffeine on glandular stomach carcinogenesis induced in rats by N-methyl-N'-nitro-N-nitrosoguanidine and sodium chloride. *Food Chem Toxicol* 1995;33:21–26.
- Lu G, Liao J, Yang G, Reuhl KR, Hao X, Yang CS. Inhibition of adenoma progression to adenocarcinoma in a 4-(methylnitrosamino)-1-(3-pyridyl)-1-butanone-induced lung tumorigenesis model in *A/J* mice by tea polyphenols and caffeine. *Cancer Res* 2006;66:11494–11501.
- Rothwell K. Dose-related inhibition of chemical carcinogenesis in mouse skin by caffeine. *Nature* 1974;252:69–70.
- Yun TK, Kim SH, Lee YS. Trial of a new medium-term model using benzo[a]pyrene induced lung tumor in newborn mice. *Anticancer Res* 1995;15:839–845.
- George KC, Hebbar SA, Kale SP, Kesavan PC. Caffeine protects mice against whole-body lethal dose of gamma-irradiation. *J Radiol Prot* 1999;19:171–176.
- Farooqi Z, Kesavan PC. Radioprotection by caffeine pre- and post-treatment in the bone marrow chromosomes of mice given whole-body gamma-irradiation. *Mutat Res* 1992;269:225–230.
- Kesavan PC, Natarajan AT. Protection and potentiation of radiation clastogenesis by caffeine: Nature of possible initial events. *Mutat Res* 1985;143:61–68.
- Lyles MB, Cameron IL, Rawls HR. Structural basis for the binding affinity of xanthenes with the DNA intercalator acridine orange. *J Med Chem* 2001;44:4650–4660.
- Davies DB, Veselkov DA, Djimant LN, Veselkov AN. Hetero-association of caffeine and aromatic drugs and their competitive binding with a DNA oligomer. *Eur Biophys J (Germany)* 2001;30:354–366.
- Evstigneev MP, Khomich VV, Davies DB. Complexation of anthracycline drugs with DNA in the presence of caffeine. *Eur Biophys J Biophys Lett* 2006;36:1–11.
- Traganos F, Kapuscinski J, Darzynkiewicz Z. Caffeine modulates the effects of DNA-intercalating drugs in vitro: A flow cytometric and spectrophotometric analysis of caffeine interaction with novantrone, doxorubicin, ellipticine, and the doxorubicin analogue AD198. *Cancer Res* 1991;51:3682–3689.
- Shoyab M. Caffeine inhibits the binding of dimethylbenz[*a*]anthracene to murine epidermal cells DNA in culture. *Arch Biochem Biophys* 1979;196:307–310.
- Telo JP, Vieira A. Mechanism of free radical oxidation of caffeine in aqueous solution. *J Chem Soc-Perkin Trans 2* 1997;1755–1757.
- Stadler RH, Richoz J, Turesky RJ, Welti DH, Fay LB. Oxidation of caffeine and related methylxanthenes in ascorbate and polyphenol-driven Fenton-type oxidations. *Free Radical Res* 1996;24:225–240.
- Zylber J, Ouazzanichahdi L, Chiaroni A, Riche C. Controlled C-5 methylation of caffeine by benzoyloxy radical-addition at C-8. *Tetrahedron Lett* 1988;29:2055–2058.
- Devasagayam TP, Kesavan PC. Radioprotective and antioxidant action of caffeine: Mechanistic considerations. *Indian J Exp Biol* 1996;34:291–297.
- Kumar SS, Devasagayam TP, Jayashree B, Kesavan PC. Mechanism of protection against radiation-induced DNA damage in plasmid pBR322 by caffeine. *Int J Radiat Biol* 2001;77:617–623.
- Tatsumi K, Sakane T, Sawada H, Shirakawa S, Nakamura T. Unscheduled DNA synthesis in human lymphocytes treated with neocarzinostatin. *Gann* 1975;66:441–444.
- Sasada M, Sawada H, Nakamura T, Uchino H. Caffeine potentiation on lethality of L-1210 cells treated with neocarzinostatin. *Gann* 1976;67:447–449.

35. Tatsumi K, Tashima M, Shirakawa S, Nakamura T, Uchino H. Enhancement by caffeine of neocarzinostatin cytotoxicity in murine leukemia L1210 cells. *Cancer Res* 1979;39:1623–1627.
36. Iseki S, Ebina T, Ishida N. Effects of caffeine on neocarzinostatin-induced inhibition of cell cycle traverse in HeLa-S3 cells. *Cancer Res* 1980;40:3786–3791.
37. Iseki S, Ebina T, Ishida N. Caffeine-induced recovery from G2 block caused by neocarzinostatin. *Gann* 1980;71:567–571.
38. Hatayama T, Yukioka M. Mode of inhibition of DNA replication in neocarzinostatin-treated HeLa cells. *Biochim Biophys Acta* 1983;740:291–299.
39. Hatayama T, Qi SL, Kim K, Ichiba K, Yukioka M. Caffeine-induced reorganization of DNA replicating system occurs on or near nuclear matrix in HeLa cells. *Biochem Int* 1984;9:651–657.
40. Iseki S, Mori T. Effect of poly(adenosine diphosphate-ribose) polymerase inhibitors on neocarzinostatin-induced G2 delay in HeLa-S3 cells. *Cancer Res* 1985;45:4224–4228.
41. Povirk LF, Goldberg IH. Stoichiometric uptake of molecular oxygen and consumption of sulfhydryl groups by neocarzinostatin chromophore bound to DNA. *J Biol Chem* 1983;258:11763–11767.
42. Kuo H-M, Lee Chao P-D, Chin D-H. Delocalized electronic structure of the thiol sulfur substantially prevents nucleic acid damage induced by neocarzinostatin. *Biochemistry* 2002;41:897–905.
43. Chin D-H, Tseng M-C, Chuang T-C, Hong M-C. Chromatographic and spectroscopic assignment of thiol induced cycloaromatizations of enediyne in neocarzinostatin. *Biochim Biophys Acta* 1997;1336:43–50.
44. Chin D-H, Li H-H, Sudhakar CG, Tsai P-Y. Insight into the strong inhibitory action of salt on activity of neocarzinostatin. *Bioorg Med Chem* 2010;18:1980–1987.
45. Dedon PC, Goldberg IH. Influence of thiol structure on neocarzinostatin activation and expression of DNA damage. *Biochemistry* 1992;31:1909–1917.
46. Povirk LF, Wubker W, Kohnlein W, Hutchinson F. DNA double-strand breaks and alkali-labile bonds produced by bleomycin. *Nucleic Acids Res* 1977;4:3573–3580.
47. Powell SN, Abraham EH. The biology of radioresistance: Similarities, differences and interactions with drug resistance. *Cytotechnology* 1993;12:325–345.
48. Povirk LF, Houlgrave CW. Effect of apurinic/aprimidinic endonucleases and polyamines on DNA treated with bleomycin and neocarzinostatin: Specific formation and cleavage of closely opposed lesions in complementary strands. *Biochemistry* 1988;27:3850–3857.
49. Chin D-H. Rejection by neocarzinostatin protein through charges rather than sizes. *Chem-Eur J* 1999;5:1084–1090.
50. Myers AG, Cohen SB, Kwon BM. DNA cleavage by neocarzinostatin chromophore: Establishing the intermediacy of chromophore-derived cumulene and biradical species and their role in sequence-specific cleavage. *J Am Chem Soc* 1994;116:1670–1682.
51. Zylber J, Zylber N, Chiaroni A, Riche C. Free-radical addition of trichloromethyl to caffeine access to C-8 polyhalogenoalkane derivatives and to unexpected 5-trichloromethyl-1,3,7 trimethyl-5,7-dihydrouric acid. *Tetrahedron Lett* 1984;25:3853–3856.
52. Kimura H, Aoyama T. Decrease in sensitivity to ethidium bromide by caffeine, dimethylsulfoxide or 3-aminobenzamide due to reduced permeability. *J Pharmacobio-Dyn* 1989;12:589–595.
53. Baranovsky SF, Bolotin PA, Evstigneev MP, Chernyshev DN. Interaction of ethidium bromide and caffeine with DNA in aqueous solution. *J Appl Spectrosc* 2009;76:132–139.
54. Hatayama T, Goldberg IH. DNA damage and repair in relation to cell killing in neocarzinostatin-treated HeLa cells. *Biochim Biophys Acta* 1979;563:59–71.
55. Kappen LS, Goldberg IH. Activation of neocarzinostatin chromophore and formation of nascent DNA damage do not require molecular-oxygen. *Nucleic Acids Res* 1985;13:1637–1648.
56. Chin D-H, Kappen LS, Goldberg IH. 3'-Formyl phosphate-ended DNA: High-energy intermediate in antibiotic-induced DNA sugar damage. *Proc Natl Acad Sci USA* 1987;84:7070–7074.
57. Lyles MB, Cameron IL. Caffeine and other xanthines as cytochemical blockers and removers of heterocyclic DNA intercalators from chromatin. *Cell Biol Int* 2002;26:145–154.
58. Nafisi S, Manouchehri F, Tajmir-Riahi HA, Varavipour M. Structural features of DNA interaction with caffeine and theophylline. *J Mol Struct* 2008;875:392–399.
59. Tornaletti S, Russo P, Parodi S, Pedrini AM. Studies on DNA binding of caffeine and derivatives: Evidence of intercalation by DNA-unwinding experiments. *Biochim Biophys Acta* 1989;1007:112–115.
60. Fritzsche H, Lang H, Sprinz H, Pohle W. On the interaction of caffeine with nucleic acids. IV. Studies of the caffeine-DNA interaction by infrared and ultraviolet linear dichroism, proton and deuterium nuclear magnetic resonance. *Biophys Chem* 1980;11:121–131.
61. Pohle W, Fritzsche H. Infrared dichroism of the DNA-caffeine complex. A new method for determination of the ligand orientation. *Nucleic Acids Res* 1976;3:3331–3335.
62. Gao X, Stassinopoulos A, Gu J, Goldberg IH. NMR studies of the post-activated neocarzinostatin chromophore-DNA complex. Conformational changes induced in drug and DNA. *Bioorg Med Chem* 1995;3:795–809.
63. Gao X, Stassinopoulos A, Rice JS, Goldberg IH. Structural basis for the sequence-specific DNA strand cleavage by the enediyne neocarzinostatin chromophore. Structure of the post-activated chromophore-DNA complex. *Biochemistry* 1995;34:40–49.
64. Gao X, Stassinopoulos A, Ji J, Kwon Y, Bare S, Goldberg IH. Induced formation of a DNA bulge structure by a molecular wedge ligand-postactivated neocarzinostatin chromophore. *Biochemistry* 2002;41:5131–5143.
65. Evstigneev MP, Rybakova KA, Davies DB. Complexation of norfloxacin with DNA in the presence of caffeine. *Biophys Chem* 2006;121:84–95.
66. Masip L, Veeravalli K, Georgiou G. The many faces of glutathione in bacteria. *Antioxid Redox Signal* 2006;8:753–762.
67. Shukla V, Gude RP. Potentiation of lipid peroxidation in B16F10 and B16F1 melanoma cells by caffeine, a methylxanthine derivative: Relationship to intracellular glutathione. *Chemotherapy* 2003;49:71–75.
68. Farag MM, Abdelmeguid EM. Hepatic glutathione and lipid-peroxidation in rats treated with theophylline—Effect of dose and combination with caffeine and acetaminophen. *Biochem Pharmacol* 1994;47:443–446.
69. Kappen LS, Ellenberger TE, Goldberg IH. Mechanism and base specificity of DNA Breakage in intact cells by neocarzinostatin. *Biochemistry* 1987;26:384–390.
70. DeGraff WG, Russo A, Mitchell JB. Glutathione depletion greatly reduces neocarzinostatin cytotoxicity in Chinese hamster V79 cells. *J Biol Chem* 1985;260:8312–8315.
71. DeGraff WG, Mitchell JB. Glutathione dependence of neocarzinostatin cytotoxicity and mutagenicity in Chinese hamster V-79 cells. *Cancer Res* 1985;45:4760–4762.